

2-D Scalable Optical Controlled Phased-Array Antenna System

Maggie Yihong Chen¹, Brie Howley², Xiaolong Wang², Panoutsopoulos Basile³ & Ray T. Chen²

¹Omega Optics Inc, 10435 Burnet Rd, Austin, TX 78758

²Microelectronics Research Center, The University of Texas at Austin, Austin, TX 78758

³Naval Undersea Warfare Center, Newport, RI 02841

ABSTRACT

A novel optoelectronically-controlled wideband 2-D phased-array antenna system is demonstrated. The inclusion of WDM devices makes a highly scalable system structure. Only (M+N) delay lines are required to control a M×N array. The optical true-time delay lines are combination of polymer waveguides and optical switches, using a single polymeric platform and are monolithically integrated on a single substrate. The 16 time delays generated by the device are measured to range from 0 to 175 ps in 11.6 ps. Far-field patterns at different steering angles in X-band are measured.

Keywords: phased-array antenna, WDM, optoelectronic, polymer, waveguide, thermo-optic, optical switch

1. INTRODUCTION

Next generation capabilities of microwave fiber optic systems include true time delay (TTD) beamforming, tunable microwave filtering, and signal processing. Radar system can benefit significantly from the low loss and EMI immune remoting, reduced size, weight and mechanical flexibility of a microwave fiber optic system. A key photonic integrated circuit module is a scalable, integrated optical delay line with fast reconfiguration time.

Many optical schemes have been proposed to take advantages of an optical feed for true-time delay, including acousto-optic (AO) integrated circuit technique [1-3], Fourier optical technique [4-6], bulky optics techniques [7-12], dispersive fiber technique [13-17], fiber grating technique [18-19], and substrate guided wave techniques [20-22]. Time delay modules utilizing the AO technique are considerably compact and integrated. However, this approach has a relatively limited bandwidth. Fourier optical technique is capable of rapid and high-resolution beam steering with only azimuth and elevation commands and no digital processing. However, this method is not a broadband true-time delay technology, because the optical frequency needs to change with the RF frequency of the antenna to maintain the correct phase ramp period for a certain steering angle. The drawbacks of the bulk optics approach are large space requirement and alignment maintenance. Increased maximum time delay will require more space, so the total size of the TTD control unit will be massive. Dispersive fiber technique is quite effective in power consumption and space consumption. However, it is relatively difficult for this technique to produce large enough time delays, since it requires excessively long dispersive delay lines. Bragg fiber grating technique can be used only for microwave signals of less than 1 GHz. The waveguide loss is a limiting factor of substrate guided wave techniques. Furthermore, when the above technologies are used in large 2-D phased-array antenna (PAA) systems, the entire system will be bulky and not practical.

We demonstrate an innovative 2-D PAA systems controlled by monolithic TTD module based on polymer platform in this paper. The inclusion of WDM devices makes a highly scalable system structure. Only (M+N) delay lines are required to control a M×N array. Offset and trench structures are introduced to reduce bending loss of waveguides. Total internal reflection (TIR) thermo-optic switches are designed and fabricated. Compact TTD devices are obtained through the monolithic integration of the TIR switches and waveguide delay lines. The delay device is then integrated into the 2-D PAA system for beam steering measurements.

2. 2-D PAA SYSTEM STRUCTURE

The scalable 2-D PAA system structure is illustrated in Fig.2.1. RF signals are injected simultaneously onto multiple-wavelength optical carriers that have been multiplexed through WDM. The signals are dynamically routed in TTD units through integrated high-speed optical switches. The PAA structure can support tens of simultaneous beams. Reconfigurability is achieved through the incorporation of the optical switch in the TTD lines. The inclusion of WDM devices makes this structure highly scalable. The delay signals are encoded by the first stage of MUX, and are decoded by the second stage of DMUX, so that only $(M+N)$ delay lines are required to control a $M \times N$ array. The optical true-time delay lines are combination of polymer waveguides and optical switches, using a single polymeric platform and are monolithically integrated on a single substrate. Due to the wide range of time delays achievable from the switched TTD lines, the phased-array antenna can support ultra-wide instantaneous bandwidth from hundreds of MHz to hundreds of GHz. We use 6 MUX/DMUX modules and 4 plus 4, totally 8 true time delay module to control a 4×4 sub-array.

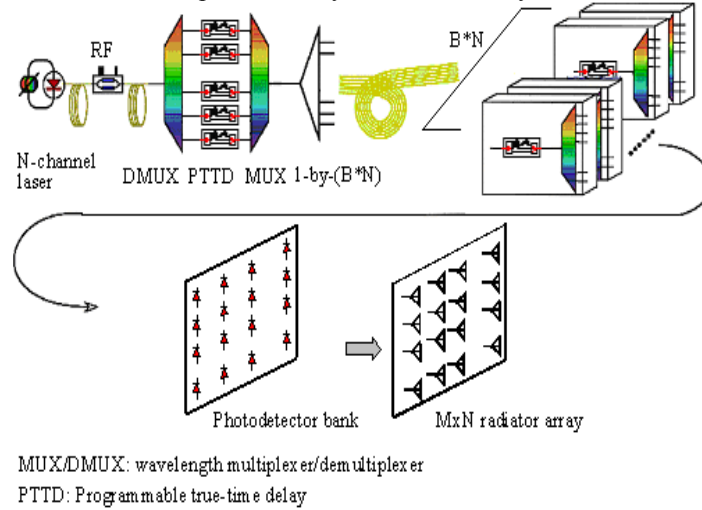


Fig.2.1 Schematic diagram of the 2-D scalable true-time delay PAA.

The optical-switch-based reconfigurable true-time delay line is detailed in Fig.2.2. Reconfigurability is built into the structure by combining the polymer waveguides and optical switches. Using optical switches, various time delay values are achieved with a minimum number of hardware devices. For example, we can achieve $2^N = 1024$ time delay values with $N = 10$ segment waveguides. The differential delay time through one TTD line is

$$T_l = \sum_{j=1}^N S_{l,j} \Delta t_j = \sum_{j=1}^N S_{l,j} 2^{j-1} \tau, \quad S_{l,j} = 0,1, \quad (1)$$

where $S_{l,j}$ is the state of the j -th optical switch in the l -th TTD unit.

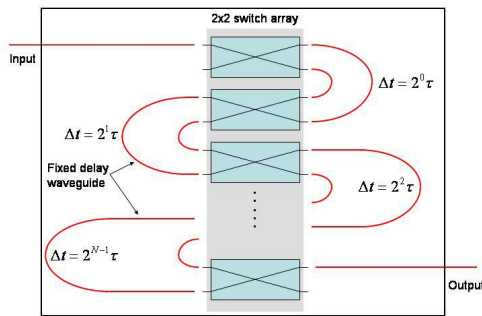


Fig.2.2 Schematic diagram of a reconfigurable true-time delay line.

3. OPTICAL TIME DELAY LINE FABRICATION

The fabrication is discussed in two parts, one is the low loss waveguide, the other is the 2x2 optical switch array.

3.1. Low bend loss curvature waveguide fabrication

In order to have a small footprint, curved waveguide must be used in the time delay circuit. There are two kinds of losses related to curved waveguides. One is the radiation loss at the junction, due to the difference of the guided modes in straight and curved waveguides. The other is power dissipation or “pure bending loss” when light travels down a bend of constant radius. To reduce the junction loss, the overlap integral of the straight segment and curved segment modes can be maximized by varying the offset between the two modes, and therefore the two segments [23], as in Fig.3.1. Placing a trench outside the curved waveguide can reduce the pure bending loss. This trench prevents light from spreading outward toward larger radii, thus improving beam confinement [24]. We took into account both of these approaches and optimize the position of waveguide offset (WO), trench offset and the size of the trench, on the delay line topology shown in Fig.3.1.

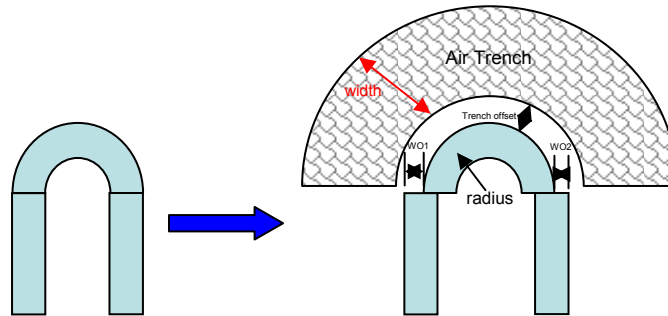


Fig.3.1 Left: Original delay line topology, right: Modified delay line structure with waveguide offset and trench.

The trench depth is 20 μm and width is 20 μm with an index of 1.0. Various trench offsets were simulated and the results are drawn in Fig. 3.2. The simulated values suggest that for bend radii greater than 4 mm the use of trenches and offsets have an insignificant effect on the insertion loss. However, for small bend radii of less than 4 mm, trenches improve the bend loss performance significantly. Based on a 7- μm trench separation, waveguide offsets were introduced and optimized. As can be seen in Fig.3.3, the waveguide offsets further decrease the propagation loss. We measured the insertion loss of a fabricated 180° bend with 1.5 mm radius. The insertion loss was reduced from 17.74 dB to 2.43 dB, with optimized waveguide offsets and an air trench. The combination of trenches and offsets can result in smaller radius bends having less insertion loss than bends with greater radii because of smaller propagation losses. For the polymer waveguides tested, the bend radius can be reduced to approximately 1.5 mm without significant increases in the loss, a 50% bend radius reduction over the standard waveguide bend.

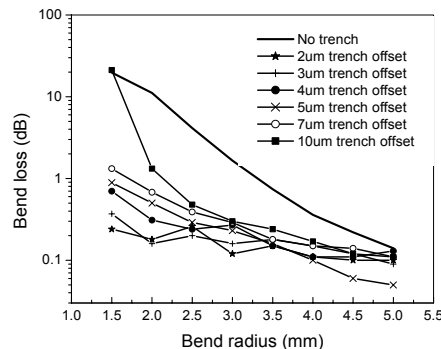


Fig.3.2 Simulated bend loss versus bend radius and trench offset.

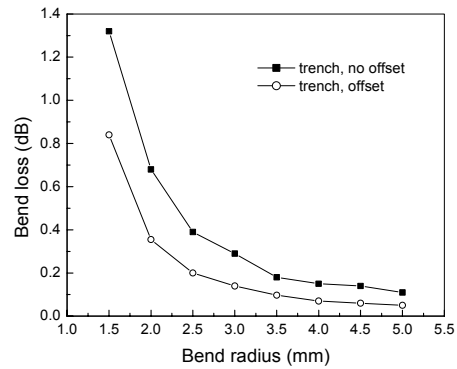


Fig.3.3 Simulated bend loss under different offset conditions.

3.2. 2x2 thermal optical (TO) switch fabrication

Fig.3.4 shows the schematic diagram of the TO total internal reflection (TIR) switch. The refractive indices of the cladding and core are 1.45 and 1.46 respectively, and the waveguide dimension is $6.5 \times 6.5 \mu\text{m}^2$. The separation between the input and output waveguide is $250 \mu\text{m}$, which is compatible with a standard fiber array. The radii of the bent waveguides are 10mm, which will cause negligible bending loss and guided mode perturbation. The bent waveguides are then connected by two tapered width waveguides to form an X junction. The electrode heater, which is formed by a thin gold film, is set at the crossing point of the symmetric X junction. Then enlarged square pads were formed to apply the current probe. Fig.3.5 (a) shows the microscopic picture of the fabricated TIR switch. Fig.3.5 (b) shows an SEM picture of a portion of the crossing waveguide after RIE. The insertion loss was measured to be 2.8dB. The switching time of the TIR switch is mainly determined by the thermal conductivity of the polymer. We used a square waveform with amplitude of 1.2V and offset at 0.6V to drive the heater and frequency at 200Hz. The optical response in the two output channels has a rise and fall time of 1.5ms and 2ms, respectively.

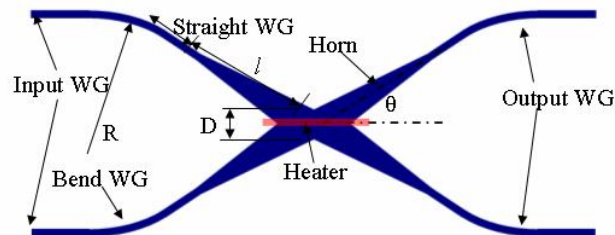


Fig.3.4 Schematic diagram of the TO TIR switch.

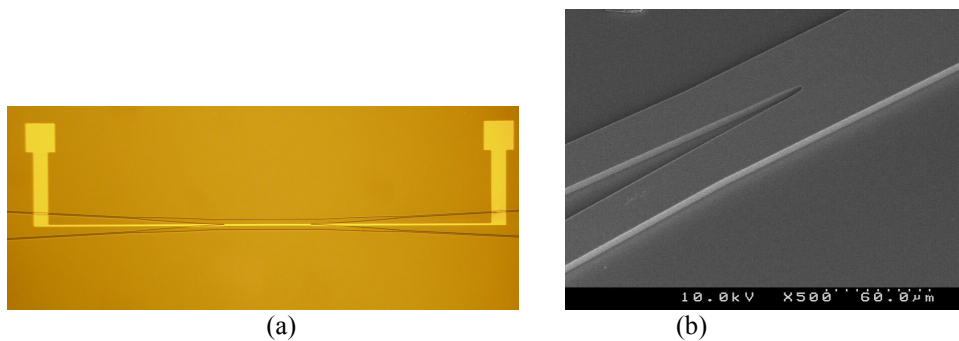


Fig.3.5 (a) microscopic picture of the TO switch (b) SEM of the crossing waveguide.

Fig.3.6 shows the optical power in the cross and bar ports as a response to the electrical driving power. The tested switch, with a half branch angle of 4° , has a crosstalk of -31dB in the cross state, and the power consumption, which is also called static power, is zero. This is a profitable feature since it can reduce the average power consumption by half in real applications. When the driving power increases, the optical power in cross port will decrease and the optical power in the bar port will increase simultaneously. Eventually, the switch will reach the bar state. Here we define the driving power at which we get maximum optical power in the bar state as the switching power. It is 44mW in Fig.3.6. The total resistance including the pads and lead lines is 48.0Ω and the resistance of the heater is 39.1Ω . The thermal efficiency is estimated to be 81.5% .

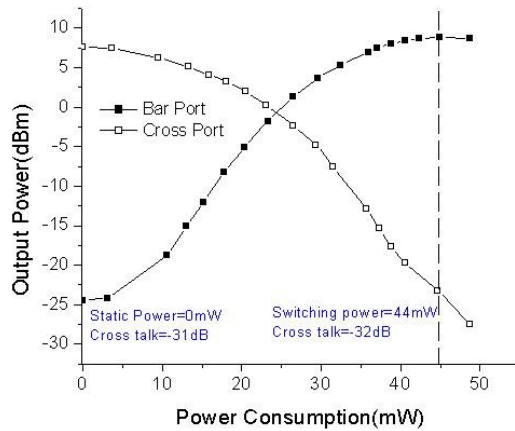


Fig.3.6 The switching characteristics of the TIR switch.

4. 4-BIT TIME DELAY DEVICE CHARACTERIZATION

The 4-bit time delay device is capable of providing 16 time delay values, measured to range from 0 to 175 ps in 11.6 ps increments. The first and the last two states are shown in Fig.4.1. We measured the time delay value of all 16 cases. Designed and measured time delay values are compared in Fig.4.2, with a maximum derivation of 1.4%.

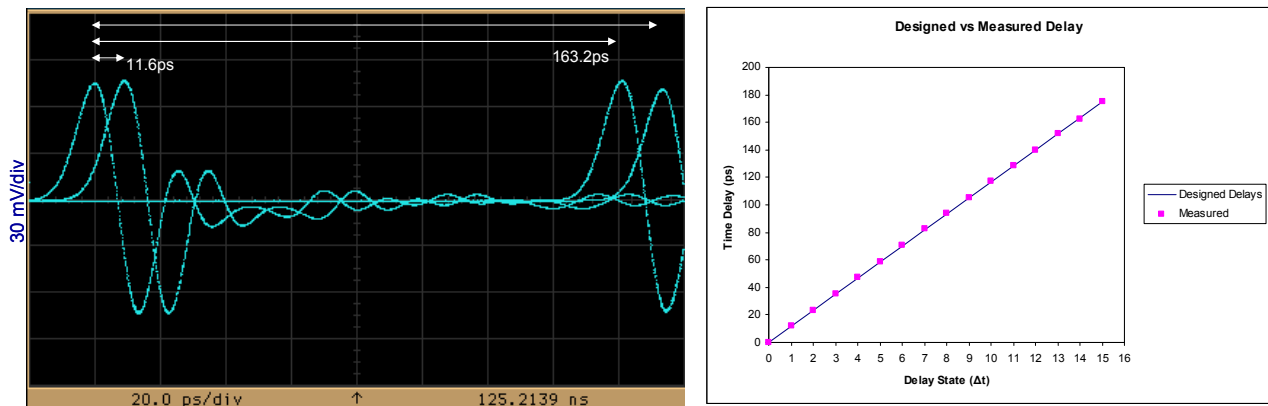


Fig.4.1 The first and the last two states. Fig.4.2 Comparison of designed and measured time delay values.

5. FAR FIELD PATTERN OF THE 2-D PAA SYSTEM

First we calibrate a 3-element sub-array at 0° . Then we program the optical switch “on” and “off” states to provide time delays for each antenna element for 15.5° and -15.5° beam steering. The measured far field patterns are shown in Figs.5.1 (a) and (b). The Figs illustrate the beam steering effect. The elements of sub-array we use are not uniform. Therefore we used the average data as the calculation data, which is shift a little bit from the demonstrated value.

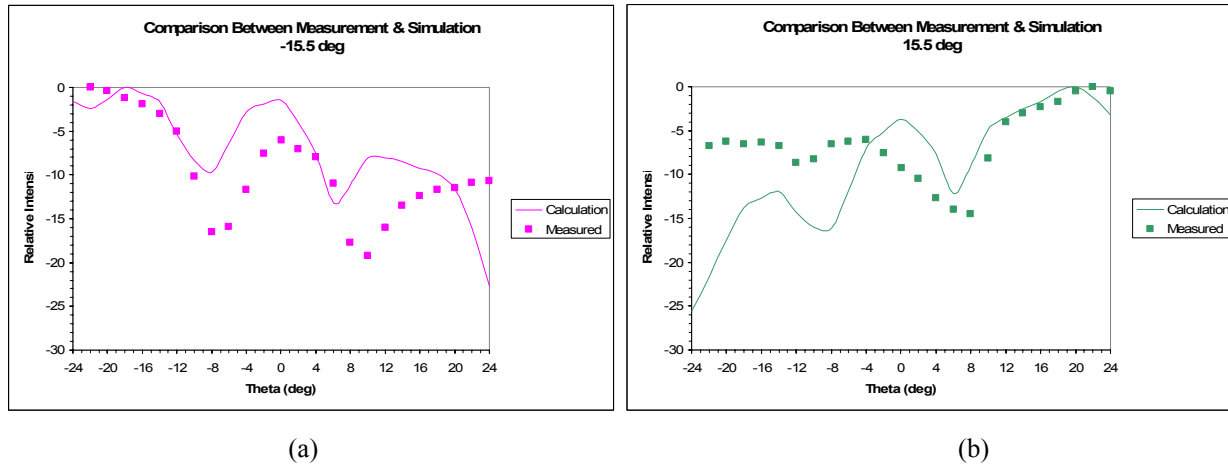


Fig. 5.1 Far field patterns at 15.5° and -15.5° .

6. CONCLUSION

A 2-D PAA system controlled by optical true time delay circuit is designed and evaluated, which dramatically reduce the number of hardware required. An optical time delay device, incorporating low loss waveguide and 2×2 TO switches, is designed and fabricated. By choosing the correct trench and offset design parameters, the bend radius of low index contrast polymer waveguides can be reduced by 50% or more. Low insertion loss optical switches are integrated on the circuit, with a switching speed of 2ms. The time delay circuit can be utilized in signal processing, radar beamforming, and various other applications.

7. REFERENCES

1. L. H. Gesell, R. E. Feinleib, J. L. Lafuse, and T. M. Turpin, “Acousto-optic control of time delays for array beam steering”, *SPIE*, vol. 2155, pp. 194, 1994.
2. Maak, P.; Frigyes, I.; Jakab, L.; Habermayer, I.; Gyukics, M.; Richter, P. “Realization of true-time delay lines based on acousto optics”, *IEEE Journal of Lightwave Technology*, Vol.20, April 2002, pp. 730 –739.
3. Nabeel A. Riza, “Acoustic-optic liquid-crystal analog beam former for phased-array antennas”, *Applied Optics*, vol. 33(17), pp. 3712-3724, 1994.
4. G. A. Koepf, “Optical processor for phased-array antenna beam formation”, *Proc. SPIE*, vol.477, 75-81, 1984.
5. L. P. Anderson, F. Boldissar, and R. Kunath, “Antenna beamforming using optical processor”, In *1987 AP-S Int.Symp. Dig.*, June 1987. pp. 431-434.
6. Yoshihiko Konishi, etc., “Carrier-to-Noise Ratio and Sidelobe Level in a Two-Laser Mode Optically Controlled Array Antenna Using Fourier Optics”, *IEEE Trans. on Antennas and Propagation*, vol. 40, pp. 1459-1465, 1992.
7. N. A. Riza, “Liquid crystal-based optical time delay control system for wideband phased arrays”, *SPIE*, 1790, 171, 1992.
8. H. R. Fetterman, Y. Chang, D. C. Scott, S. R. Forrest, F. M. Espiau, M. Wu, D. V. Plant, J. R. Kelly, A. Mather, W. H. Steier, R. M. Osgood, H. A. Haus, and G. J. Simonis, “Optically controlled phased array radar receiver using SLM switched real time delays”, *IEEE Microwave Guid. Wave Lett.* 5, 414–416, 1995.

9. X. S. Yao and L. Maleki, "A novel 2D programmable photonic time delay device for millimeter wave signal processing applications", *IEEE Photon. Technol. Lett.* 6, 1463–1465, 1994.
10. I. Frigyes and A. J. Seeds, "Optically generated true-time delay in phased array antennas", *IEEE Trans. Microwave Theory Tech.* 43, 2378–2386, 1995.
11. J. Fu, M. Schamschula, and H. J. Caulfield, "Modular solid optic time delay system", *Opt. Commun.* 121, 8–12, 1995.
12. D. Dolfi, P. Joffre, J. Antoine, J.-P. Huignard, D. Philippet, and P. Granger, "Experimental demonstration of a phased-array antenna optically controlled with phase and time delays", *Applied Optics*, Vol. 35, No. 26, 1996.
13. D.T.K. Tong and M.C. Wu, "Multiwavelength Optically Controlled Phased- Array Antennas", *IEEE Trans. On Microwave and Tech.* Vol. 46, No.1, pp. 108-115, 1998.
14. M. Y. Frankel, R. D. Esman, and M. G. Parent, "Array transmitter/receiver controlled by a true time-delay fiber-optic beamformer", *IEEE Photon. Technol. Lett.*, vol. 7, pp. 1216–1218, Oct. 1995.
15. A. Goutzoulis and K. Davies, "Development and field demonstration of a hardware-compressive fiber-optic true-time delay steering system for phased-array antennas", *Opt. Eng.*, vol. 3, pp. 8173–8185, Dec. 1994.
16. J. Lembo, T. Holcomb, M. Wickham, P. Wisseman, and J. C. Brock, "Low-loss fiber optic time-delay element for phased-array antennas", in *Proc. SPIE-Int. Soc. Opt. Eng.*, vol. 2155, pp. 13–23, 1994.
17. Y. Chang, B. Tsap, H. R. Fetterman, D. A. Cohen, A. F. Levi, and I. L. Newberg, "Optically controlled serially fed phased-array transmitter", *IEEE Microwave Guided Wave Lett.*, vol. 7, pp. 69–71, Mar. 1997.
18. Molony A., Edge C., and Bennion I., "Fiber grating time delay element for phased array antennas," *Elec. Lett.*, vol.31, 1485-1486, 1995.
19. Cruz, J. L. etc, "Chirped fiber gratings for phased-array antennas", *Electron. Lett.*, 1997, 33(7), pp. 545-546.
20. Yihong Chen, Xuping Zhang, Ray T. Chen, "Substrate-Guided-Wave Hologram Based Continuously Variable True-Time-Delay Module for Microwave Phased-Array Antennas", *SPIE proceeding of Optoelectronic interconnection*, 2002
21. Yihong Chen, Ray T. Chen, "A fully Packaged True Time Delay Module for a K-band Phased Array Antenna System Demonstration", *IEEE Photonic Technology Letter*, Vol.14, pp.1175-1177, 2002
22. Yihong Chen, and Ray T. Chen, "K-band Phased-Array Antenna System Demonstration using Substrate Guided Wave True-Time Delay", *Optical Engineering*, Vol. 42, No. 7, pp. 2000-2005, July 2003
23. E. G. Neumann, "Curved dielectric optical waveguide with reduced transition losses," *IEE Proc.*, 129, pt. H, pp. 278-300, 1982.
24. "Low loss dielectric optical waveguide bends," *Fiber and Integr. Optics*, 4, 2, pp. 203-211, 1982.